

FACULTY OF ENGINEERING
ALEXANDRIA UNIVERSITYAlexandria University
Alexandria Engineering Journalwww.elsevier.com/locate/aej
www.sciencedirect.com

ORIGINAL ARTICLE

On the performance of circular concrete-filled high strength steel columns under axial loading

Mohamed Mahmoud El-Heweity*Structural Engineering Department, Faculty of Engineering, Alexandria University, Egypt*

Received 16 May 2012; revised 26 May 2012; accepted 27 May 2012

Available online 4 July 2012

KEYWORDSAxial strength;
Ductility;
Confinement;
Concrete-filled steel columns;
Finite element technique

Abstract This work presents a numerical study to investigate the performance of circular high-strength steel tubes filled with concrete (CFT) under monotonic axial loading. A model is developed to implement the material constitutive relationships and non-linearity. Calibration against previous experimental data shows good agreement. A parametric study is then conducted using the model and compared with codes provisions. Strength and ductility of confined concrete are of primary concern. Variables considered are yield stress of steel tube and column diameter. The assessment of column performance is based on axial load carrying capacities and enhancements of both strength and ductility due to confinement. Two parameters namely strength enhancement factor (K_f) and ductility index (μ) are clearly defined and introduced for assessment. Results indicate that both concrete strength and ductility of CFT columns are enhanced but to different extents. The ductile behaviors are significantly evident. The increase in yield stress of steel tube has a minimal effect on concrete strength but pronounced effect on concrete ductility. However, reduction in ductility is associated with using high-tensile steel of Grade 70. The overall findings indicate that the use of high-strength tube in CFT columns is not promising. This finding may seriously be considered in seismic design.

© 2012 Faculty of Engineering, Alexandria University. Production and hosting by Elsevier B.V.
All rights reserved.**1. Introduction**

Cold-formed steel tubular members have become popular in seismic regions, especially, for high rise structures [1]. Tests have been performed by Walpole [2], Jain et al. [3], Sherman

and Sully [4] and Grzebieta et al. [5] on cold-formed hollow section members. The results showed that the capacity of cold-formed tubular members reduced significantly due to local buckling in the sections and the magnitude of the local buckles became tremendous under quasi-static or cyclic loading.

At that point, concrete filled steel tube (CFT) columns were introduced and used to improve the load carrying capacity, ductility and to prevent or delay local buckling of tubular sections under different loading history. Actually, CFT columns comprise of two different materials with distinctly different behavior especially that concrete is neither homogeneous nor

E-mail address: ugss_alexandria@yahoo.com

Peer review under responsibility of Faculty of Engineering, Alexandria University.



Production and hosting by Elsevier

isotropic material. Hence, the failure mechanism depends to large extent on the shape, length, diameter, and tube's thickness, in addition to concrete and steel grades. Other parameters such as steel-concrete bond, concrete confinement, residual stresses, creep, shrinkage, and type of loading may also have pronounced effect [6–11]. Many investigations on CFT columns were reported elsewhere [7–24] where numerical and experimental studies on the behavior of CFT columns for different shapes, dimensions and material strengths were explored.

The confinement effect introduced by the steel tube in the concrete core is an important aspect of the structural behavior of CFT columns. According to Susantha et al. [25], Shanmugam and Lakshmi [26], and Sakino et al. [16], the confinement mechanism in the early stages of loading is minimal and can be neglected, since the Poisson coefficient of the concrete is smaller than the steel Poisson's coefficient. Therefore, the steel tube expands faster than the concrete core in the radial direction and the steel tube does not restrain the concrete core. At this point, no separation does exist between the steel and the adjacent concrete. However, when the applied load reaches the uniaxial strength of concrete, the concrete microcracking initiates and propagates. The concrete lateral expansion reaches its maximum, mobilizing the steel tube and efficiently confining the concrete core. The ultimate capacity of the CFT columns is therefore higher than the sum of the resistance of their components. The radial stress introduced by the steel tube on concrete is responsible for the additional resistance of the concentrically loaded CFT columns where the concrete core is subjected to a triaxial stress state and the steel tube is under a biaxial stress state [27].

On the other hand, results reported by numerous researchers [6–19] showed that the beneficial effect of confinement on improving strength and ductility is affected by other parameters such as the diameter-to-thickness ratio (D/t), length-to-diameter ratio (L/D), eccentricity of the load (e/D), strength and stiffness of the materials, and cross configuration. It is of interest to recognize that the analyses of these previous studies did not mostly differentiate between the possible difference in the degrees of enhancements in strength and ductility as affected by studied parameters. The urgent need of such information in case of CFT columns is essential especially for high steel grades.

2. Research significance

Ductility and strength are among the improved features of concrete-filled steel tubular column. In such cases, the beneficial effect of concrete confinement is well known; however, the degree of efficiency of steel tube with different grades to enhance the brittle performance of concrete is still a matter of arguments among researchers. From general prospective, it is believed that higher yield stress of steel tube is preferable for confinement mechanism. Actually, this may not be true for both strength and ductility. The most adequate steel grade required for improving strength or ductility may be differ and is obviously questionable. This point is directly addressed herein. This paper provides investigation of this subject using a powerful finite-element software package 'ANSYS' [28]. The work highlights on the axial deformation and failure behavior of steel-concrete assembly. The study provides useful information about the degree of enhancement in both concrete strength and ductility as affected by the column diameter

and yield stress of steel as well. The current study may serve as a basis for cost consuming introducing in Egypt. The assessment of different variables is explored. The work concludes performance-based guidelines that may be useful in codes provisions and may seriously be considered for columns subjected to seismic-type loading.

3. Finite element model

3.1. Finite element type and mesh

Owing to the thin-walled nature of the steel tube, shell elements were employed to model the steel tube. The four-node shell element with reduced integration SHELL181 has been utilized in this study. This element has six degrees of freedom per node and provides an accurate solution to most applications. The mesh was chosen to be relatively coarse based on the studies of Wu [29] who recognized that the mesh refinement has very little influence on the numerical results. For concrete core, three dimensional eight-node solid elements, so called SOLID65, was used. To simulate the bond between the steel tube and the concrete core, the contact interaction model in ANSYS [28] is utilized. A surface-based interaction with a contact pressure-over closure model in the normal direction, and a Coulomb Friction Model in the tangential direction to the surface, are used. In order to construct contact between two surfaces, the slave and master surfaces must be chosen successfully. Generally, if a smaller surface contacts a larger surface, the best is to choose the smaller surface as the slave surface. If the distinction cannot be made, the master surface should be chosen as the surface of the stiffer body or as the surface with the coarser mesh if the two surfaces are on structures with comparable stiffness. The stiffness of the structure and not just the material should be considered when choosing the master and slave surface. Herein, the steel tube is less stiff than the concrete core even though the steel material has a higher stiffness than the concrete material. Therefore, the steel surface is chosen as the slave surface whereas the concrete core surface is chosen as the master surface.

3.2. Material constitutive models

CFT columns comprised of steel and concrete materials. The uniaxial behavior of the steel tube can be simulated by an elastic-perfectly plastic model with an associated flow rule. When the steel tube is subjected to multiple stresses, a von Mises yield criterion, F , is employed to define the elastic limit, which is written as

$$F = \sqrt{3J_2} = \frac{1}{\sqrt{2}} \sqrt{(\sigma_1 - \sigma_2)^2 + (\sigma_2 - \sigma_3)^2 + (\sigma_3 - \sigma_1)^2} = \sigma_y \quad (1)$$

where J_2 is the second stress invariant of the stress deviator tensor and σ_1 , σ_2 , and σ_3 are the principal stresses.

For concrete core, circular CFT columns with small D/t ratios provide high considerable confinement for the concrete. In this case, an equivalent uniaxial stress-strain relationship for confined concrete should be used. On the other hand, high D/t ratios provide inadequate confinement for the concrete, therefore the uniaxial stress-strain relationship for unconfined concrete should be used. Mander et al. [30] defined the limiting

D/t , ratio between confined and unconfined concrete to be equal to 29.2. In this model, Poisson's ratio, ν_c , in the elastic part of concrete under uniaxial compression stress is taken equals to 0.2 according to ASCE [31]. Fig. 1 presents the equivalent uniaxial stress–strain curve for confined concrete, as well as the unconfined stress–strain concrete curve [30]. Three parts of the curve have to be identified in the case of confined concrete. The value of ε_c is taken equals 0.003 as suggested by ACI Committee 318/318R [32]. The confined concrete strength, f_{cc} , and the corresponding strain, ε_{cc} , may be calculated from equations:

$$f_{cc} = f_c + k\sigma_{lat} \quad (2)$$

$$\varepsilon_{cc} = \varepsilon_c \left(1 + \frac{5\sigma_{lat}}{f_c} \right) \quad (3)$$

where f_c , ε_c and σ_{lat} represent the unconfined concrete strength, corresponding strain and the confining pressure around the concrete core, respectively.

Because the concrete in the CFT columns is usually subjected to tri-axial compressive stresses, the failure of concrete is dominated by the compressive failure surface, expanding with increasing hydrostatic pressure. Hence, a linear Drucker–Prager yield criterion is used to model the yield surface of concrete. The first part of the curve is assumed to be an elastic part up to the proportional limit, which is taken as $0.5f_{cc}$. The initial modulus of elasticity, E_{cc} , is highly correlated to its compressive strength and can be calculated from the empirical equation of ACI Committee 318/318R [32] as follows:

$$E_{cc} = 4700\sqrt{f_{cc}} \text{ in MPa} \quad (4)$$

The second part of the curve is the nonlinear portion, starting from the proportional limit stress, $0.5f_{cc}$, to the confined concrete strength, f_{cc} . The stress–strain relationship proposed by Saenz [33] has been widely adopted as the uniaxial stress–strain curve for concrete and it has the following form:

$$f_c = \frac{E_{cc}\varepsilon}{1 + (R + R_E - 2)\left(\frac{\varepsilon}{\varepsilon_c}\right) - (2R - 1)\left(\frac{\varepsilon}{\varepsilon_c}\right)^2 + R\left(\frac{\varepsilon}{\varepsilon_c}\right)^3} \quad (5)$$

where $R = \frac{R_E(R_\sigma - 1)}{(R_E - 1)^2} - \frac{1}{R_E}$, $R_E = \frac{E_{cc}\varepsilon_c}{f_{cc}}$ and $R_\sigma = 4$, $R_\varepsilon = 4$ may be used, as recommended by Hu and Schnobrich [34].

In the analysis, Eq. (5) is taken as the equivalent uniaxial stress–strain curve for concrete when the concrete strain, ε , is less than ε_{cc} , as can be seen in Fig. 1. When $\varepsilon > \varepsilon_{cc}$, a linear descending line (the third part of the curve) is used to model

the softening behavior of concrete. If k_3 is defined as the material degradation parameter, the descending line is assumed to be terminated at the point where $f_c = rk_3f_{cc}$ and $\varepsilon = 11\varepsilon_{cc}$. To account for the effect of different concrete strengths, the degradation parameter, k_3 , should be multiplied by an additional reduction factor, r , which is taken as 1.0 for $f_{cu} = 30$ MPa and 0.5 for $f_{cu} \geq 100$ MPa with linear interpolation for f_{cu} between 30 and 100 MPa. On the other hand, the values of the parameters σ_{lat} and k_3 are determined by matching the numerical results with the experimental data.

3.3. Boundary conditions and load application

The concrete-filled steel column is modeled as pinned-roller member. Due to symmetry, only on fourth of the column is analyzed. Symmetric displacement boundary conditions are defined for the nodes along the two planes of symmetry. A uniform distributed load is applied statically at the top of the upper end of the column using a thick plate using the displacement control. The load is applied in increments using the Arc-Length method available in the ANSYS library. Fig. 2 shows the finite element mesh and the boundary conditions of the analyzed CFT column.

4. Verification of the developed model

The results of the developed model using the nonlinear finite element program ANSYS [28] is calibrated against experimental data. Table 1 summarizes the material properties and geometries of six CFT columns reported by Schneider [10] and Huang et al. [14]. The comparisons are given below in Fig. 3.

Fig. 3 shows the axial load versus axial strain for the six verified CFT columns using the proposed model in conjunction with the experimental results of Schneider [10] and Huang et al. [14]. The figure clearly demonstrates that the model is capable of predicting the load–strain relationship of the investigated CFT columns with good accuracy. It is obvious from the curves that the results are in good agreement with the experimental data. It is strongly believed that the developed model provides good opportunity to outline trends in the behavior of CFT columns under axial loads as affected by different parameters. The model is therefore used in the coming section to study the pre-selected variables affecting the performance of CFT columns.

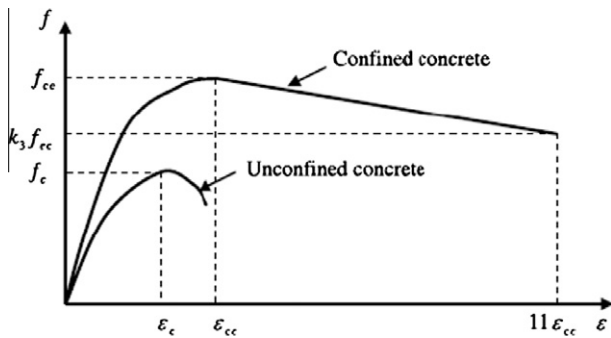


Figure 1 Equivalent uniaxial stress–strain curve for confined concrete [30].

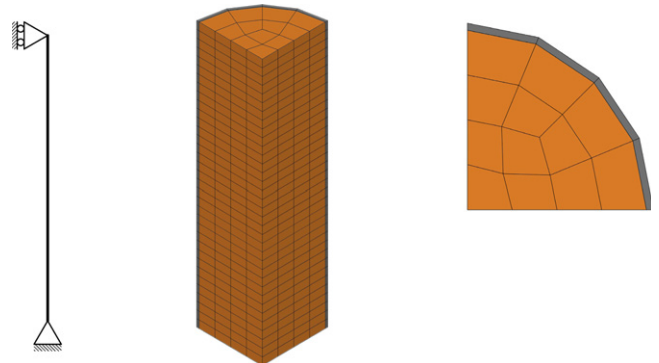


Figure 2 Finite element model of the analyzed CFT column.

Table 1 Geometrical and material properties of selected CFT columns.

Ref.	CFT designation	Dimensions (mm)			Ratios		Material properties	
		D	t	L	D/t	L/D	f_{cu} (MPa)	f_y (MPa)
Schneider [10]	C-01	140	6.5	602	22	4.3	23.80	313.0
	C-02	140	3.0	602	47	4.3	28.18	285.0
	C-03	300	3.0	900	100	3.0	27.23	232.0
Huang et al. [14]	C-04	200	5.0	840	40	4.2	27.15	265.8
	C-05	280	4.0	840	70	3.0	31.15	272.6
	C-06	300	2.0	840	150	2.8	27.23	341.7

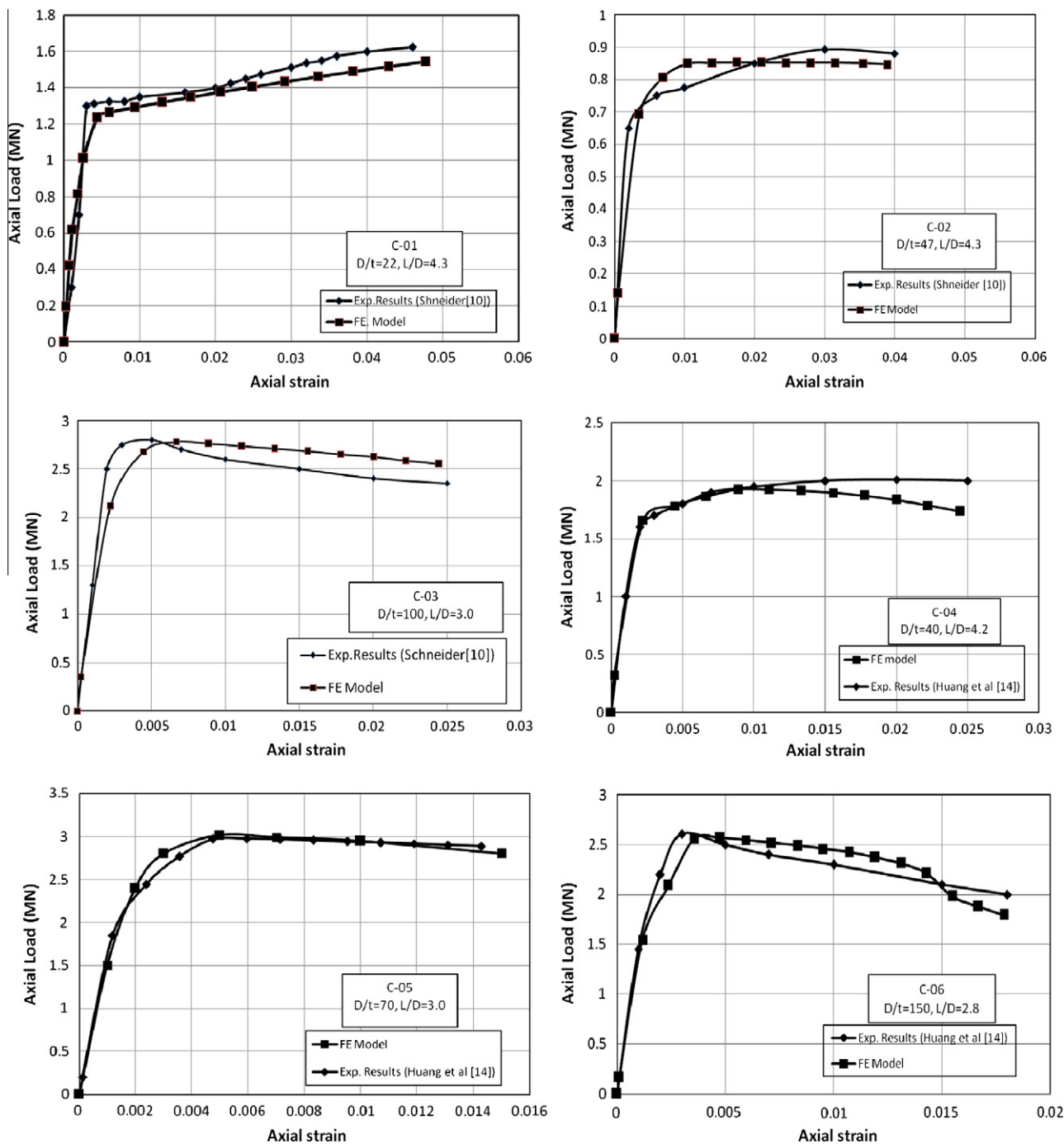


Figure 3 Verification of the developed model.

5. Parametric study

The parametric study is conducted using the model on nine circular CFT columns to investigate the effect of two main parameters on columns performances. The load carrying capacity and ductility of CFT columns are explored. The first examined parameter is the yield stress of the steel case. Three yield stress values equal to 240, 360 and 520 MPa are considered. The second parameter is the column diameter that is taken equal to 100, 140 and 200 mm.

It should be pointed out that all analyzed CFT columns have circular cross-section with diameter to length ratio, L/D equals to 3, and diameter to thickness ratio, D/t equals to 50. The compressive strength of the unconfined concrete, f_c is kept constant at a value of 30 MPa, while the concrete elastic modulus is taken as, $E_{cc} = 20$ GPa. Poisson’s ratio of concrete is assumed throughout the study to remain at its minimum value of $\nu_c = 0.20$ to attain the minimum level of confinement contribution. It is believed that this assumption should be adopted to ensure conservative design.

6. Results and discussions

The numerical results of studied columns are listed in Table 2 while the axial load carrying capacity versus axial strain for all columns is illustrated in Figs. 4–6. The effects of column diameter and yield stress of tubular steel on confinement effectiveness with respect to strength and ductility are critically explored and presented graphically in Figs. 7–15. The subsections below discuss the effect of the studied parameters.

6.1. Capacity aspects

The failure mode of the analyzed columns was identified as fully material plasticity of the steel tube. It was noticeable herein that the mode of failure of CFT columns was not changed by changing both studied parameters. On the other hand, Figs. 4–6 depict that the axial load decreased slowly in the post-peak region, indicating reasonable ductility performance for CFT columns. Large columns with diameter 200 mm could not undergo relatively large axial strain (0.032) as compared to a strain of 0.046 achieved by smaller columns (100 mm in diameter).

It should be pointed out that the maximum axial carrying capacity in CFT column increases with increasing the column

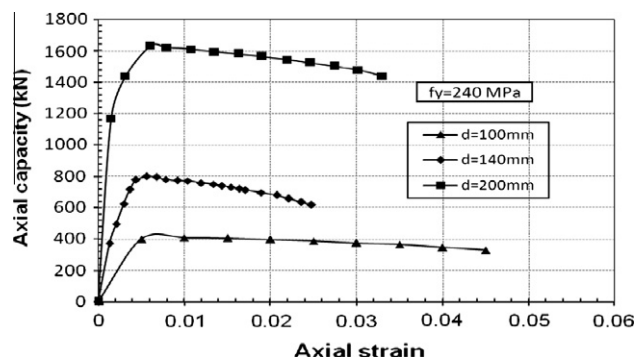


Figure 4 Load–strain response of CFT columns with different diameter sizes and for $f_y = 240$ MPa.

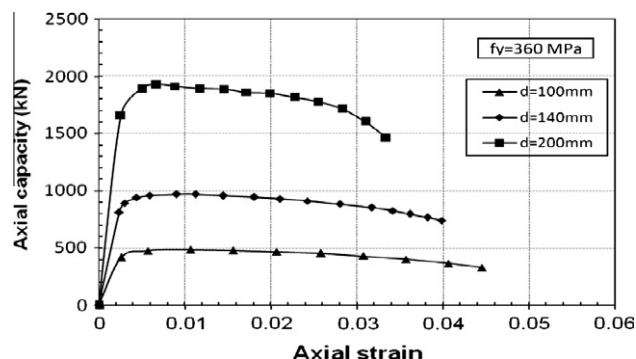


Figure 5 Load–strain response of CFT columns with different diameter sizes and for $f_y = 360$ MPa.

diameter as also seen in Table 2 and Fig. 7. Generally, increasing the diameter much increases both stiffness and capacity. For example, when the diameter increases from 100 mm to 140 mm (40%), the axial capacity of the column improves by up to 95%. Actually, this improvement may be due to increasing the yield stress of steel case which leads to much confinement to the concrete core. Besides, increasing the yield stress of the steel case increases its vertical contribution to the axial ultimate capacity of CFT column. Furthermore, the results show that for the same column diameter that the axial capacity, P_{FE} , increases by 18% and 42% as the steel yield stress increases from 240 MPa to 360 MPa and 520 MPa, respectively.

Table 2 Computed axial capacities, P_{FE} , of the analyzed CFT columns.

CFT	Steel yield stress (MPa)	Dimensions (mm)			Ratios		Axial capacities, P_{FE} (kN)
		D	t	L	D/t	L/D	
CFT-01	240	100	2.0	300	50	3	411.4
CFT-02		140	2.8	420			774.1
CFT-03		200	4.0	600			1617.8
CFT-04	360	100	2.0	300			486.2
CFT-05		140	2.8	420			940.6
CFT-06		200	4.0	600			1913.9
CFT-07	520	100	2.0	300			584.8
CFT-08		140	2.8	420			1140.4
CFT-09		200	4.0	600			2309.7

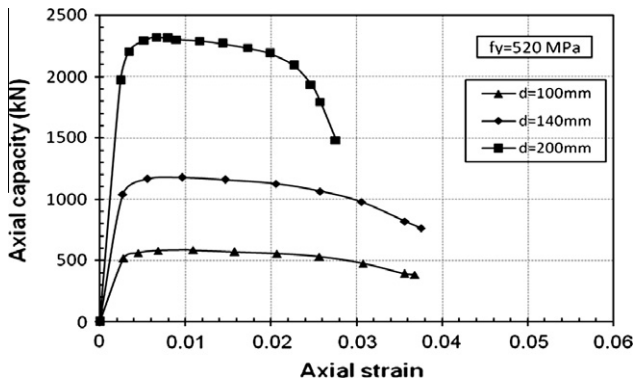


Figure 6 Load-strain response of CFT columns with different diameter sizes and for $f_y = 520$ MPa.

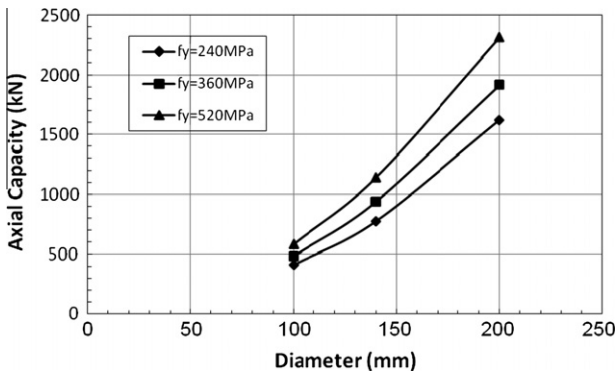


Figure 7 Effect of column diameter and steel yield stress on axial capacities of CFT columns.

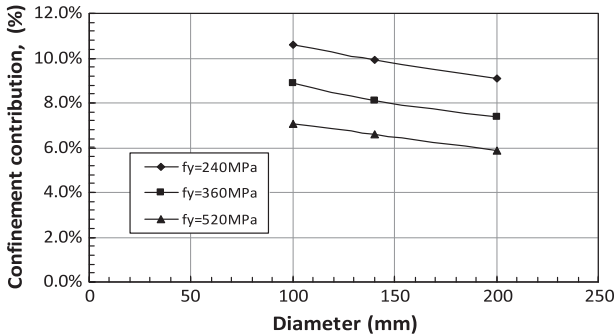


Figure 8 Effect of column diameter and steel yield stress on confinement contribution for axial capacities of CFT columns.

From another point of view, the confinement contribution on the axial carrying capacity of CFT columns is calculated by subtracting the contribution of steel case and concrete core column from the total axial capacity determined by the developed model. Hence, the confinement contribution, ψ , may be written as

$$\psi = (P_{FE} - (f_y \times A_s + f_c \times A_c)) \times 100 / P_{FE} \quad (6)$$

Fig. 8 shows that increasing the diameter of column decreases the confinement contribution on the axial capacity of CFT column. Meanwhile, increasing the yield stress of the steel

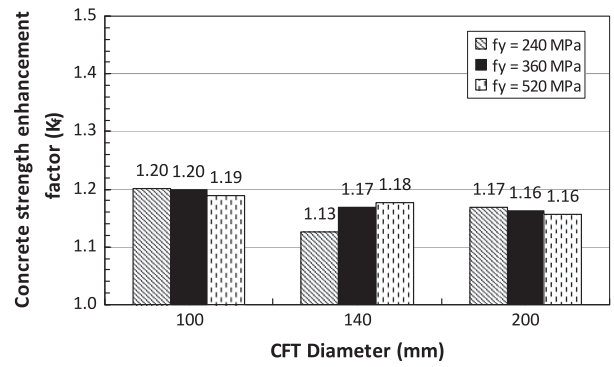


Figure 9 Effect of CFT column diameter on the degree of concrete strength enhancement for different steel yield stresses.

case increases the confinement contribution of CFT column. For example, the share of the confinement contribution is 10.6%, 9.9% and 9.1% for steel yield stress, $f_y = 240$ MPa and diameter size equals 100, 140 and 200 mm, respectively. On the other hand, for steel yield stress, $f_{ey} = 520$ MPa the share of the confinement contribution is 7.0%, 6.6% and 5.9% for the same diameter sizes. Strength and ductility aspects are discussed latter sections.

6.2. Strength aspects

The improvement in concrete strength due to the developed confining pressure may be seen in Fig. 9 where the strength enhancement factor designated as (K_f) is plotted against the column diameters for different values of steel yield. The term K_f simply represents the ratio between the strength of confined concrete (f_{cc}) to the strength of unconfined concrete (f_c). The term f_{cc} is determined using the following expression:

$$F_{cc} = [P_{FE} - A_s \times f_y] / A_c \quad (7)$$

where A_s and f_y are the cross-sectional area and the yield stress of steel tube, while A_c is the cross-sectional area of the concrete core.

The figure clearly demonstrates that all enhancement factors (K_f) associated with a specified column diameter are comparable. However, slightly differences are noticeable for columns with different sizes. Based on the argument mentioned above, it can be concluded that the use of steel tube with high yield stress as generally believed is not necessary. An improvement on the order of 20% can be achieved by utilizing low steel grade. It is also clear from the figure that the average K_f for column with diameter 100 mm is about 1.20 while it goes slightly down to 1.16 for larger column with diameter 200 mm. This finding implies that higher concrete volume may need slightly higher confinement to attain the same level of strength improvement.

From general prospective, it can be stated that the variables examined herein may have no effect on the strength enhancement of confined concrete. An improvement about 20% is always governed. This finding agrees with similar trend reported by Rochette and Labossiere [35] who found that excessive confinement was not very effective and improvement of maximum stress may not be achieved. At this stage, introducing ductility may raise a critical issue.

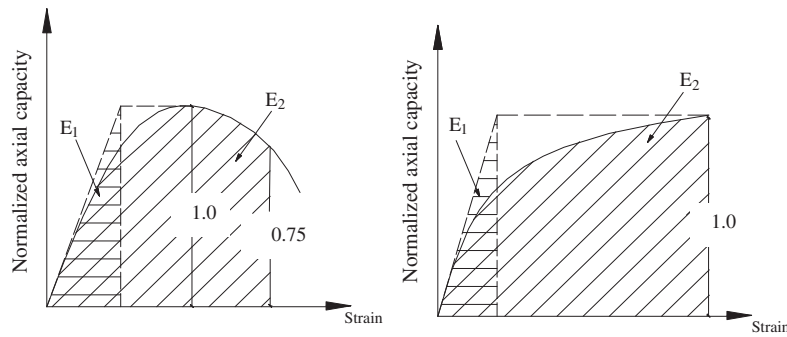


Figure 10 Definitions of ductility parameters E_1 and E_2 .

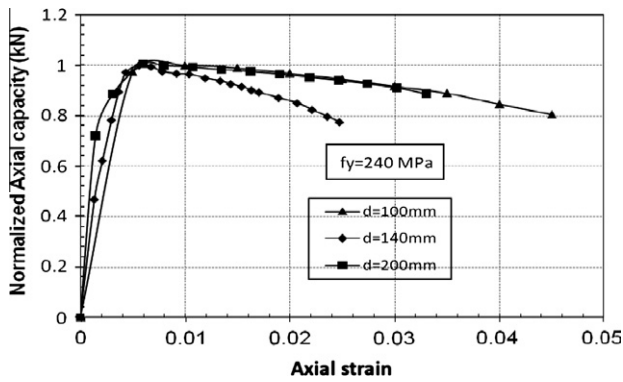


Figure 11 Normalized load–strain curve of CFT columns with different diameter sizes and for $f_y = 240$ MPa.

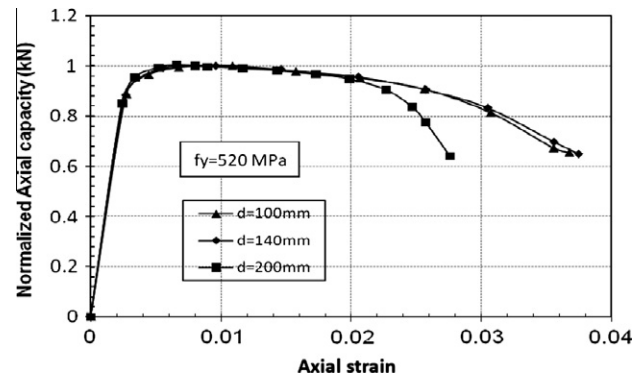


Figure 13 Normalized load–strain curve of CFT columns with different diameter sizes and for $f_y = 520$ MPa.

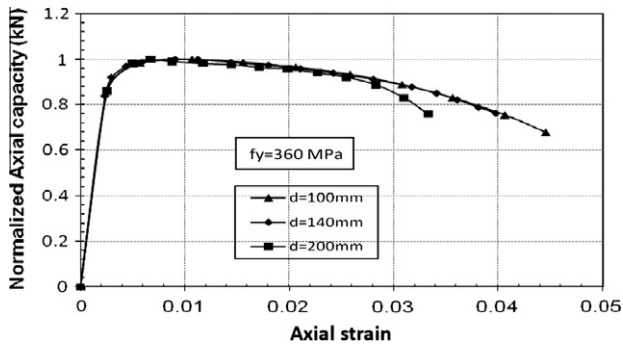


Figure 12 Normalized load–strain curve of CFT columns with different diameter sizes and for $f_y = 360$ MPa.

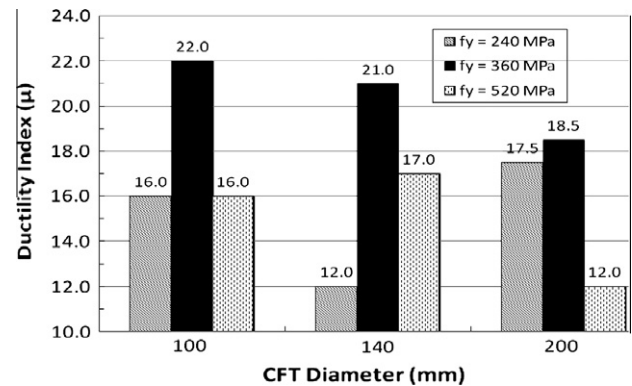


Figure 14 Effect of CFT column diameter on ductility index for different steel yield stresses.

6.3. Ductility aspects

Ductility may be easily defined in case of elasto-plastic behavior-materials; however, in concrete with a lack of such characteristic there is no universal definition for ductility. Thus, in evaluating the ductility performance of the subject CFT columns and study the effects of different variables, a parameter namely ‘Ductility Index μ ’ is adopted similarly to that previously reported elsewhere [36]. It is expressed herein as

$$\mu = E_2/E_1 \tag{8}$$

where E_2 is the area underneath normalized axial load–strain curve up to failure or 25% loss in capacity whichever comes

first, and E_1 is the area underneath the idealized curve up to the elastic limit as shown in Fig. 10.

This ductility index ‘ μ ’ is assumed to provide a reasonable basis for consistent evaluation of CFT column response and can represent the ability of the assembly to undergo large deformation while maintaining its capacity or a significant portion of it. It simply represents the ability of the composite column to absorb energy by post elastic deformation. The normalization of the axial capacity in the index gives a good basis for comparative purposes between various columns with different parameters. The higher is the ductility index the

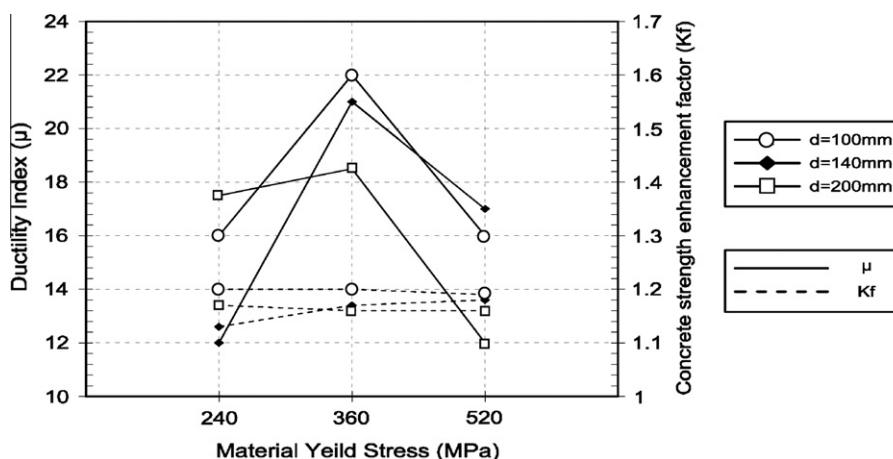


Figure 15 Ductility index (μ and strength enhancement factor (K_f) as affected by steel yield stress.

better is the column performance. The normalized axial capacity-strain curves are therefore constructed and illustrated in Figs. 11–13.

The values of the two calculated energy parameters namely ' E_1 ' and ' E_2 ' in addition to the ductility index ' μ ' are listed in Table 3. Results indicates that the ductility index ' μ ' in the studied CFT columns vary from 12 to 22 throughout the program.

The differences in the values of ductility parameters among the columns emphasize the role of yield stress of steel tube in improving the concrete ductility. Generally, the effect of column diameter on column ductility can be neglected while the effect of yield stress of steel tube on ductility is pronounced. However, no clear trend can be found. It is of interest to state that the highest ductile performance was noticeable where steel 52 having yield stress of 360 MPa was utilized. For column with diameter 100 mm, the index ' μ ' reach values of 16, 22, and 16 for steel with yield stresses of 240, 360, and 520 MPa. This implies that the ductility of lesser yield stress (360 MPa) is able to reach about 1.35 times higher than the ductility level in comparable but with tube having higher yield stress (520 MPa). Similar finding may be seen in other columns with larger diameters as seen in Fig. 14. It seems that increasing the yield stress of tube from 240 MPa to 360 MPa is essential; however, higher yield stress seems to be ineffective with respect to ductility and to cost. Introducing the cost at this stage raises a critical issue.

6.4. Strength-ductility interaction

It is strongly believed that strength and ductility of CFT columns may not necessarily affected by any parameter following similar trends. This statement seems to be true with respect to the yield stress of tube that is plotted herein in Fig. 15 against both Index ' μ ' and Factor ' K_f ' for all studied columns. The figure clearly demonstrates that the optimum yield value for ductility is 360 MPa. Higher yield adversely affects column ductility. Contradictory, strength improvement on the order of 20% can be attained by even the mild steel tube. This confirms the finding mentioned earlier. Therefore, it is very advisable in the area of construction to select the adequate steel type based on studied basis.

6.5. Cost aspects

It is strongly believed that strength and ductility of CFT columns may not necessarily. At this stage, the construction of Fig. 16 raises a critical issue. The figure correlates both price and strength enhancement factor (K_f) of each CFT column (on the right y axis) to the ductility index (μ) (on the left y axis) as affected by the yield stress of steel tube. The subject yield stresses are 240 MPa (Grade 37), 360 MPa (Grade 52) and 520 MPa (Grade 70), and their commercial prices are 6000, 6700 and 14,000 Egyptian pounds per ton (LE/ton).

Table 3 Ductility index for studied CFT columns.

CFT	Steel yield stress (MPa)	Idealized elastic area (E_1)	Idealized total area (E_2)	Ductility index (μ)
CFT-01	240	0.00240	0.03840	16
CFT-02		0.00144	0.01728	12
CFT-03		0.00145	0.02538	17.5
CFT-04	360	0.00143	0.03146	22
CFT-05		0.00146	0.03066	21
CFT-06		0.00144	0.02664	18.5
CFT-07	520	0.00146	0.02336	16
CFT-08		0.00138	0.02346	17
CFT-09		0.00141	0.01692	12

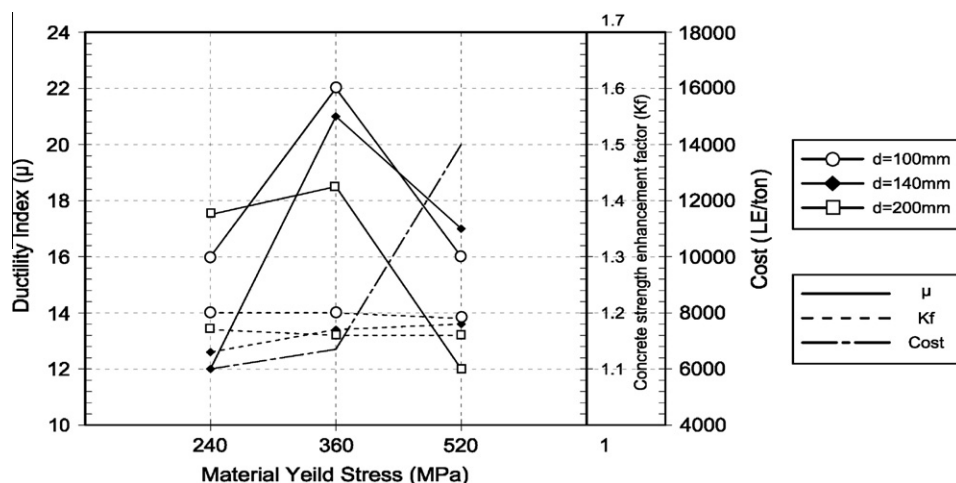


Figure 16 Simple cost inquiry.

Table 4 Comparisons of axial capacities computed by design codes and developed model.

CFT column designation	Steel yield stress (MPa)	Dimensions (mm)			Ratios		Comparisons, P_{code}/P_{FE}		
		D	t	L	D/t	L/D	P_{AISC}/P_{FE}	P_{EC4}/P_{FE}	P_{ECPSC}/P_{FE}
CFT-01	240	100	2.0	300	50	3	0.941	0.979	0.778
CFT-02		140	2.8	420			0.984	1.013	0.820
CFT-03		200	4.0	600			0.916	0.929	0.765
CFT-04	360	100	2.0	300	50	3	0.948	0.981	0.809
CFT-05		140	2.8	420			0.938	0.958	0.809
CFT-06		200	4.0	600			0.912	0.917	0.788
CFT-07	520	100	2.0	300	50	3	0.954	0.984	0.839
CFT-08		140	2.8	420			0.938	0.951	0.833
CFT-09		200	4.0	600			0.905	0.900	0.806
Mean							0.9376	0.9569	0.8052
COV (%)							2.56	3.80	3.05

As evident from the graph, the strength factor K_f of the composites are comparable regarding the price, while the ductility index are completely different giving 16, 22, and 16 for 100 mm-columns, 12, 21, and 17 for 140 mm-columns, and finally 17.5, 18.5, and 12 for 200 mm-columns. It can therefore be concluded that the price of steel itself does no reflect its capability for improving neither column ductility nor concrete strength. Again, the selection of the appropriate steel type must ultimately base on the needed target.

7. Comparison with code provisions

Codes provisions are introduced to calculate the load carrying capacity of CFT columns under concentric loads. Results obtained through the current study and three different design codes [37–39] are compared in Table 4. These codes are AISC/LRFD [37], Eurocode 4 (EC4) [38] and ECPSC/LRFD [39]. In fact, these codes present different expressions to predict the load carrying capacity of CFT columns. Regardless the pro and burden of such approaches, the most vital issue is that these codes provisions do not give ductility due importance.

Table 4 shows the ratios between the values predicted by codes formulas and results of current research. The comparison clearly indicates that AISC and EC4 design formulas are

in good agreement with developed model. Meanwhile, ECPCS/LRFD design formula gives conservative results for all studied parameters as compared with the finite element results. It should be noted that in all calculations of the design codes formulas listed in Table 4, the resistance factors and material factors are set to one.

8. Conclusions

Based on the research presented here, the following conclusions can be drawn:

1. A numerical study on the performance of circular high-strength steel tubes filled with concrete (CFT) under monotonic axial loading is presented. A powerful finite element technique using ‘ANSYS Software’ is utilized. The prime concern is to evaluate the strength and ductility of confined concrete in the concrete–steel assembly. The two parameters namely strength enhancement factor (K_f) and ductility index (μ) are clearly defined herein and introduced as powerful tools for assessment.
2. Behavior of concrete is significantly modified due to confinement provided by the presence of external steel tube.

3. The ductile behaviors of all examined CFT columns are evident from the obtained load-versus-strains plots under axial loading. Actually, the columns responses show different trend that are much better than the typical brittle response of unconfined concrete columns that exhibits sudden collapse without any signs of warning. The ductility index (μ) of CFT columns vary from 12 to 22 as compared to a typical value of 4 for comparable unconfined concrete.
4. The enhancement on concrete strength represented by the proposed parameter K_f due to confinement seems to be within 18–20% regardless the yield stress of steel tube. This finding implies that the use of steel tube with high yield stress as generally believed is not necessary.
5. Smaller columns exhibit slightly higher concrete strength enhancement providing that the yield stress of steel tubes are comparable.
6. The increase in yield stress has a minimal effect on concrete strength. It should be pointed out that the degree of strength enhancement of concrete confined by steel tube is still a point of debate among researchers.
7. The enhancement in ductility of CFT columns is more pronounced when using steel tube of Grade 52 as compared to Grade 37 and Grade 70. In fact, increasing the yield strength of steel tube from 240 MPa (Grade 37) to 360 MPa (Grade 52) leads to significant improvement in concrete ductility. As expected, the improvement becomes pronounced for small sized-columns (up to 70% improvement). Large columns with diameter 200 mm could not undergo relatively large axial strain (0.032) as compared to a strain of 0.046 achieved by smaller columns (100 mm in diameter).
8. Further increase in yield stress of steel tubes raises a very critical aspect. For comparable column sizes, the use of steel Grade 70 ($f_y = 530$ MPa) leads to significant reduction up to 70% in concrete ductility when compared to those attained when using steel Grade 52 ($f_y = 360$ MPa) but without affecting concrete strength. In fact, the reductions in ductility that is associated with the use of high-tensile steel ($f_y = 520$ MPa) is embarrassing.
9. From the overall prospective, it may be concluded based on verified theoretical evidences that the effect of yield stress of steel tube in CFT columns on improving the concrete ductility is more significance than its effect on increasing the axial load carrying capacity of the column.
10. The improvement in concrete strength when using steel tube with yield strength higher than 240 MPa does not deserve the addition cost when compared to those achieved by higher steel grades.
11. The overall findings indicate that the use of high-strength tube in CFT columns for improving concrete ductility or strength is not promising. Low steel grade seems to be adequate. This finding may seriously be considered for columns subjected to seismic-type loading.
12. The results clearly indicate that the most reasonable steel grade for the purpose of ductility seems to be Grade 52 while any steel grade may be appropriate for the purpose of strength. From general potential, it is very advisable in the area of construction to state that the selection of the appropriate steel type must ultimately base on the needed target.

13. Finally and not least, the design formula proposed by most codes provisions gives conservative results with respect to the column axial capacity; however, regardless the pro and burden of such approaches, the attained ductility levels for CFT columns are not addresses.

References

- [1] Z. Liu, S. Goel, Cyclic load behavior of concrete-filled tubular braces, *Journal of Structural Engineering*, ASCE 114 (7) (1988) 1488–1506.
- [2] W. Walpole, Behavior of cold-formed steel RHS members under cyclic loading, in: *Proc. Tech. Conf. National Society for Earthquake Engineering*, New Zealand Society for, Earthquake Engineering, 1995.
- [3] A. Jain, S. Goel, R. Hanson, Hysteretic cycles of axially loaded steel members, *Journal of Structural Engineering*, ASCE 106 (8) (1980) 1777–1795.
- [4] D. Sherman, R. Sully, Tubular bracing member under cyclic loading, in: *Proc. 4th Pacific Structural Steel Conf.*, Singapore Society of Steel Structures, Singapore, 1994.
- [5] R. Grzebieta, X. Zhao, F. Purza, Multiple low cycle fatigue of SHS tubes subjected to gross pure bending, in: *Proc. 5th Int. Colloquium on Stability and Ductility of Steel Structures*, Univ. of Nagoya, Nagoya, Japan, 1997, pp. 847–854.
- [6] R. Furlong, Strength of steel-encased concrete beam-columns, *Journal of Structural Engineering*, ASCE 93 (5) (1967) 113–124.
- [7] M. Tomii, K. Sakino, Experimental studies on the ultimate moment of concrete filled square steel tubular beam-columns, *Transportation and Architectural Institution Japan* 275 (1979) 55–63.
- [8] H. Nakai et al., Experimental study on ultimate strength and ductility of concrete-filled thin-walled steel box columns under seismic load, *Journal of Structural Engineering*, Japan Society Civil Engineering 40A (1994) 1401–1412.
- [9] T. Fujimoto, I. Nishiyama, A. Mukai, T. Baba, Test results of eccentrically loaded short columns—square CFT columns, in: *2nd Joint Tech. Coordinating Committee Meeting (JTCC) on Composite and Hybrid Structures*, Hawaii, 1995, pp. 26–28.
- [10] S.P. Schneider, Axially loaded concrete-filled steel tubes, *Journal of Structural Engineering*, ASCE 124 (10) (1998) 1125–1138.
- [11] T. Kitada, Ultimate strength and ductility of state-of-the-art concrete-filled steel bridge piers in Japan, *Engineering Structures* 20 (4–6) (1998) 347–354.
- [12] W. Zhang, B. Shahrooz, Comparison between ACI and AISC for concrete-filled tubular columns, *Journal of Structural Engineering*, ASCE 125 (11) (1999) 1213–1223.
- [13] B. Uy, Strength of concrete filled steel box columns incorporating local buckling, *Journal of Structural Engineering*, ASCE 126 (3) (2000) 341–352.
- [14] C. Huang, Y. Yeh, H. Hu, K. Tsai, Y. Weng, S. Wang, M. Wu, Axial load behavior of stiffened concrete-filled steel columns, *Journal of Structural Engineering*, ASCE 128 (9) (2002) 1222–1230.
- [15] H. Hu, C. Huang, M. Wu, Y. Wu, Nonlinear analysis of axially loaded concrete-filled tube columns with confinement effect, *Journal of Structural Engineering*, ASCE 129 (10) (2003) 1322–1329.
- [16] K. Sakino, H. Nakahara, S. Morino, I. Nishiyama, Behavior of centrally loaded concrete-filled steel-tube short columns, *Journal of Structural Engineering*, ASCE 130 (2) (2004) 180–188.
- [17] G. Giakoumelis, D. Lam, Axial capacity of circular concrete-filled tube columns, *Journal of Constructional Steel Research* 60 (7) (2004) 1049–1068.
- [18] R. Knowles, R. Park, Strength of concrete filled tubular columns, *Journal of Structural Engineering*, ASCE 95 (12) (1969) 2565–2587.

- [19] R. Knowles, R. Park, Axial load design for concrete filled steel tubes, *Journal of Structural Engineering*, ASCE 96 (10) (1970) 2125–2153.
- [20] Bridge, R. *Concrete-Filled Steel Tubular Columns*, vol. CE18, *Civil Eng. Trans.*, Institution of Engineers, Australia, 1976, pp. 127–133.
- [21] H. Shakir-Khalil, J. Zeghiche, Experimental behavior of concrete filled rolled rectangular hollow section columns, *Structural Engineering* 67 (9) (1989) 346–353.
- [22] K. Cederwall, B. Engstrom, M. Grauers, High strength concrete used in composite columns, in: *Proc. 2nd Int. Symp. on Utilization of High-Strength Concrete*, American Concrete Institute (ACI), Detroit, 1991, pp. 195–214.
- [23] H. Shakir-Khalil, Tests on concrete-filled hollow section columns, in: *Proc. 3rd Int. Conf. on Steel–Concrete, Composite Structures*, 1991.
- [24] L. Han, G. Yao, Z. Tao, Behaviors of concrete-filled steel tubular members subjected to combined loading, *Journal of Thin Walled Structures* 45 (2007) 600–619.
- [25] K. Susantha, H. Ge, T. Usami, A capacity prediction procedure for concrete filled steel columns, *Journal of Earthquake Engineering* 5 (4) (2001) 483–520.
- [26] N. Shanmugam, B. Lakshmi, State of the art report on steel–concrete composite columns, *Journal of Constructional Steel Research* 57 (10) (2001) 1041–1080.
- [27] W. de Oliveira, S. Nardin, dC. El Debsa, M. El Debsa, Influence of concrete strength and length/diameter on the axial capacity of CFT columns, *Journal of Constructional Steel Research* 65 (2009) 2103–2110.
- [28] ANSYS, Swanson Analysis Systems Online manual, Version 10.0, and Theory Reference.
- [29] M. Wu, Numerical analysis of concrete filled steel tubes subjected to axial force. MS thesis, Dept. of Civil Engineering, National Cheng Kung University, Taiwan, 2000.
- [30] J.B. Mander, M.J.N. Priestley, R. Park, Theoretical stress–strain model for confined concrete, *Journal of Structural Engineering*, ASCE 114 (8) (1988) 1804–1823.
- [31] ASCE Task Committee on Concrete and Masonry Structure, State of the Art Report on Finite Element Analysis of Reinforced Concrete, ASCE, New York, 1982.
- [32] ACI-318/318R, *Building Code Requirements for Reinforced Concrete*, ACI, Detroit (MI), 2009.
- [33] L. Saenz, Discussion of equation for the stress–strain curve of concrete by P. Desayi, S. Krishnan, *ACI Journal* 61 (1964) 1229–1235.
- [34] H. Hu, W. Schnobrich, Constitutive modeling of concrete by using non-associated plasticity, *Journal of Materials in Civil Engineering*, ASCE 1 (4) (1989) 199–216.
- [35] P. Rochette, P. Labossiere, Axial testing of rectangle column models confined with composites, *Journal of Composites for Construction*, ASCE 4 (3) (2000) 129–136.
- [36] A. Elkurdi, S. Houry, A. Eldarwish, A. Khalifa, A. Morsy, Behavior of axially loaded columns strengthened with carbon fiber reinforced polymers, in: *Proc. 5th International Alexandria Conference for Structural and Geotechnical Engineering*, December 2003, pp. MT 351–MT 372.
- [37] AISC, *Load and Resistance Factor Design (LRFD) Specification for Structural Steel Buildings*, American Institute of Steel Construction, Chicago (IL, USA), 2005.
- [38] Eurocode 4, *Design of Composite Steel and Concrete Structures. Part 1.1: General Rules and Rules For Buildings*, EN 1994-1-1, European Committee for Standardization, British Standards Institution; 2009.
- [39] ECP-LRFD: *Load and Resistance Factor Design*, 205-MD No. 359-2007, Permanent Committee for the Code of Practice for Steel Construction and Bridges, 2009.